Article

Molecular Cell

Chromatin-Bound MDM2 Regulates Serine Metabolism and Redox Homeostasis Independently of p53

Graphical Abstract

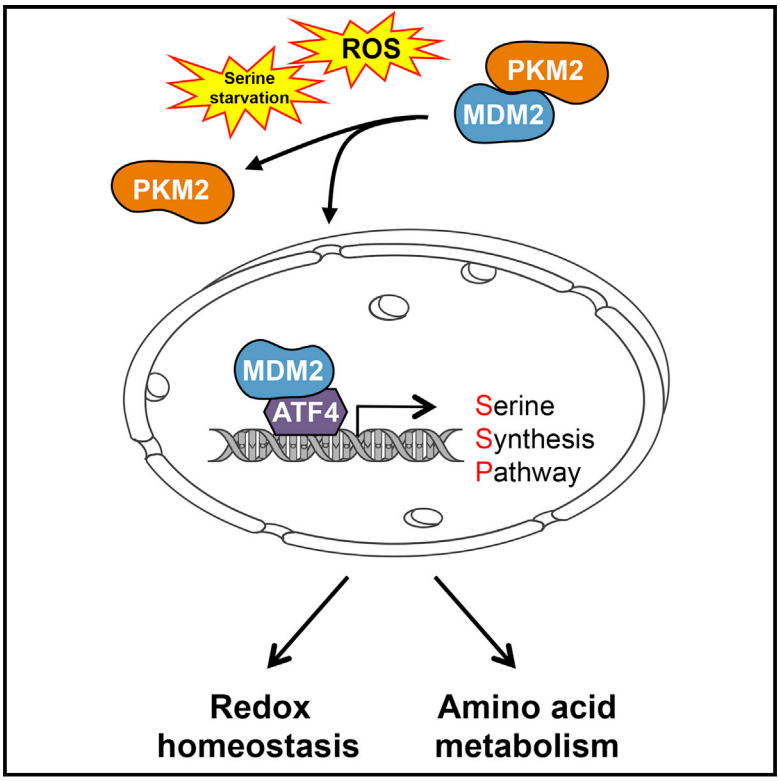

Authors

Romain Riscal, Emilie Schrepfer, Giuseppe Arena, ..., Jean-Emmanuel Sarry, Laurent Le Cam, Laetitia K. Linares

Correspondence

laurent.lecam@inserm.fr (L.L.C.), laetitia.linares@inserm.fr (L.K.L.)

In Brief

Riscal et al. show that the proto-oncogene MDM2 is recruited to chromatin through direct binding to ATF4 but independently of its well-known partner, p53. Chromatin-bound MDM2 regulates a transcriptional program involved in amino acid metabolism and redox homeostasis that contributes to cancer cell proliferation and tumor growth.

Highlights

- MDM2 is recruited to chromatin independently of p53
- Chromatin-bound MDM2 regulates amino acid metabolism and redox homeostasis
- PKM2 modulates MDM2 phosphorylation and its recruitment to chromatin
- Metabolic functions of MDM2 contribute to cancer cell proliferation

Accession Numbers

GSE64439

Riscal et al., 2016, Molecular Cell 62, 890–902
June 16, 2016
http://dx.doi.org/10.1016/j.molcel.2016.04.033

CellPress

Molecular Cell
Article

Chromatin-Bound MDM2 Regulates Serine Metabolism and Redox Homeostasis Independently of p53

Romain Riscal,[1,2,3,4] Emilie Schrepfer,[1,2,3,4] Giuseppe Arena,[1,2,3,4] Madi Y. Cissé,[1,2,3,4] Floriant Bellvert,[5,6,7] Maud Heuillet,[5,6,7] Florian Rambow,[8,9] Eric Bonneil,[10] Frédérique Sabourdy,[11,12] Charles Vincent,[1,2,3,4] Imade Ait-Arsa,[1,2,3,4] Thierry Levade,[11,12] Pierre Thibaut,[10,13] Jean-Christophe Marine,[8,9] Jean-Charles Portais,[5,6,7] Jean-Emmanuel Sarry,[12] Laurent Le Cam,[1,2,3,4,14,*] and Laetitia K. Linares[1,2,3,4,14,*]

[1]IRCM, Institut de Recherche en Cancérologie de Montpellier, 34298 Montpellier, France
[2]INSERM, U1194, 34298 Montpellier, France
[3]Université de Montpellier, 34298 Montpellier, France
[4]Institut Régional du Cancer Montpellier, 34298 Montpellier, France
[5]INSA, UPS, INP, Université de Toulouse, 135 Avenue de Rangueil, 31 077 Toulouse, France
[6]INRA, UMR792 Ingénierie des Systèmes Biologiques et des Procédés, 31400 Toulouse, France
[7]CNRS, UMR5504, 31400 Toulouse, France
[8]Laboratory for Molecular Cancer Biology, Center for the Biology of Disease, VIB, 3000 Leuven, Belgium
[9]Laboratory for Molecular Cancer Biology, Center for Human Genetics, KU Leuven, 3000 Leuven, Belgium
[10]Institute for Research in Immunology and Cancer, Université de Montréal, P.O. Box 6128 Station Centre-Ville, Montreal, QC H3C 3J7, Canada
[11]Laboratoire de Biochimie Métabolique, IFB, CHU Purpan, 31059 Toulouse, France
[12]INSERM UMR 1037, CRCT, Université Paul Sabatier Toulouse-III, 31062 Toulouse, France
[13]Department of Chemistry, Université de Montréal, P.O. Box 6128 Station Centre-Ville, Montreal, QC H3C 3J7, Canada
[14]Co-senior author
*Correspondence: laurent.lecam@inserm.fr (L.L.C.), laetitia.linares@inserm.fr (L.K.L.)
http://dx.doi.org/10.1016/j.molcel.2016.04.033

SUMMARY

The mouse double minute 2 (MDM2) oncoprotein is recognized as a major negative regulator of the p53 tumor suppressor, but growing evidence indicates that its oncogenic activities extend beyond p53. Here, we show that MDM2 is recruited to chromatin independently of p53 to regulate a transcriptional program implicated in amino acid metabolism and redox homeostasis. Identification of MDM2 target genes at the whole-genome level highlights an important role for ATF3/4 transcription factors in tethering MDM2 to chromatin. MDM2 recruitment to chromatin is a tightly regulated process that occurs during oxidative stress and serine/glycine deprivation and is modulated by the pyruvate kinase M2 (PKM2) metabolic enzyme. Depletion of endogenous MDM2 in p53-deficient cells impairs serine/glycine metabolism, the NAD^+/NADH ratio, and glutathione (GSH) recycling, impacting their redox state and tumorigenic potential. Collectively, our data illustrate a previously unsuspected function of chromatin-bound MDM2 in cancer cell metabolism.

INTRODUCTION

The MDM2 oncoprotein is an essential component of the p53 pathway that is frequently overexpressed in several types of human cancers (Biderman et al., 2012; Wade et al., 2013). The antagonistic actions of MDM2 toward p53 are mediated by its E3 ligase activity that targets p53 protein for proteasome-mediated degradation, the control of its subcellular localization, and through direct inhibition of p53 transactivation domains. The critical role of MDM2 in p53 regulation was genetically demonstrated by the rescue of the embryonic lethality of *Mdm2*-deficient mice by the concomitant inactivation of *p53* (Jones et al., 1995; Montes de Oca Luna et al., 1995). Mutations of the p53 tumor suppressor are usually mutually exclusive with other cancer-promoting genetic hits leading to MDM2 deregulation. This genetic feature of most human cancers has provided a rationale for the development of therapeutic strategies aimed at reactivating the cytotoxic functions of p53 by pharmacological agents targeting the MDM2-p53 interaction in tumors bearing wild-type p53 (Khoo et al., 2014; Li and Lozano, 2013; Saiki et al., 2015). However, evidence in both human tumors and mouse models supports the notion that MDM2 oncogenic functions extend beyond p53 regulation. Thus, some human tumors harbor both MDM2 overexpression and p53 mutations (Cordon-Cardo et al., 1994; Watanabe et al., 1994), and MDM2-overexpressing mice in a p53-null background exhibit an increased incidence of sarcomas relative to p53 knockout (KO) mice (Jones et al., 1998). These p53-independent functions of MDM2 remain poorly characterized, but several proteins with known links to cancer development have been identified as direct interactors or substrates of its E3 ligase activity (Bohlman and Manfredi, 2014; Marine and Lozano, 2010).

The mechanisms by which the p53 pathway suppresses tumorigenesis have been mainly attributed to its ability to control genome integrity and induce cell death, cell-cycle arrest, or cellular senescence (Toledo and Wahl, 2006). However, growing evidence supports the notion that the implication of p53 in

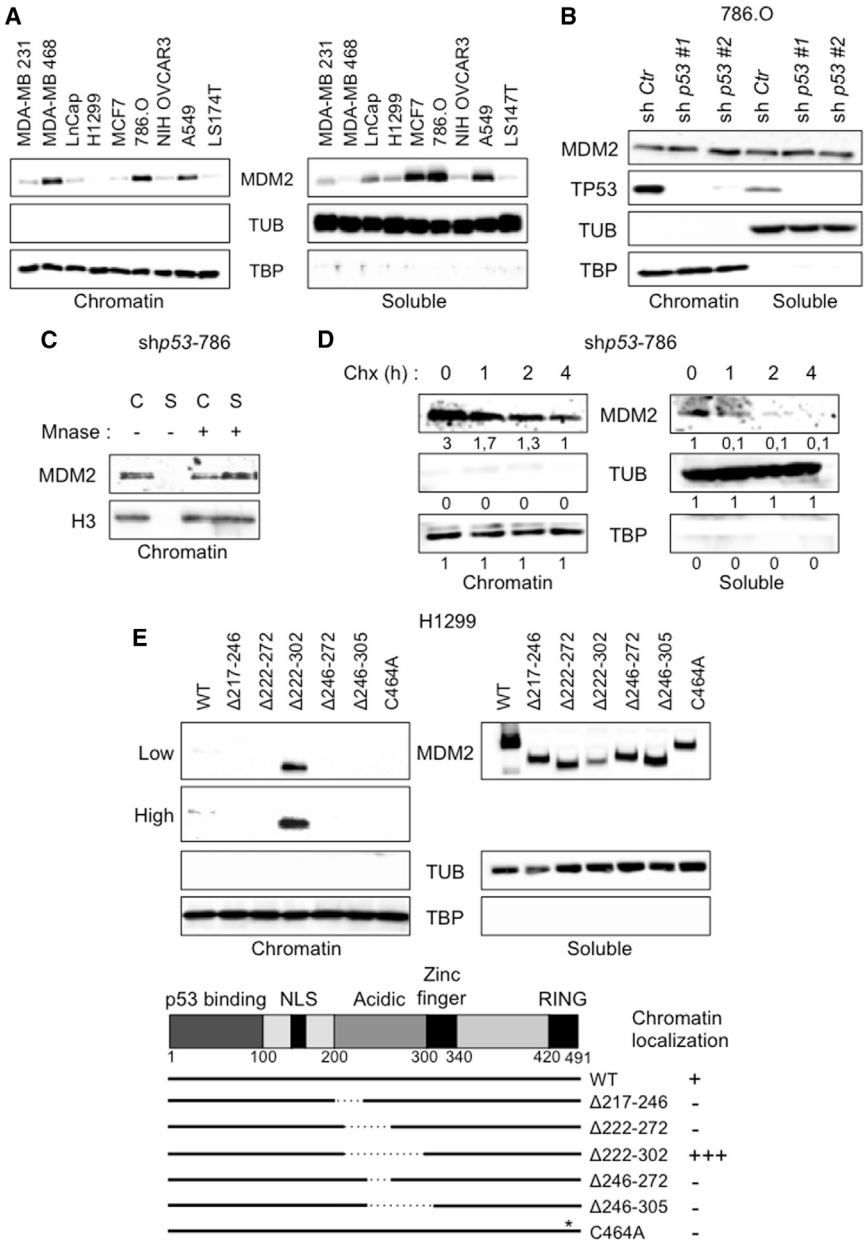

Figure 1. Mdm2 Is Localized in Chromatin Independently of p53

(A) Localization of endogenous MDM2 was assessed in different cancer cell lines by cellular fractionation methods. Fractions enriched in chromatin-associated proteins (chromatin) were separated from pooled fractions containing nucleo- and cytosoluble proteins (soluble) and analyzed by immunoblotting. The quality of the fractionation and equal loading was verified by Tata binding protein (TBP) and Tubulin (TUB) levels.

(B) Immunoblot analyses of the indicated proteins in 786.0 cells expressing a control- or *p53*-(sh*p53*-786) shRNAs after chromatin fractionation assays.

(C) Chromatin-bound MDM2 was solubilized after digestion of DNA of the chromatin fraction (C) by micrococcal nuclease (Mnase; 10 min) and recovered in the supernatant (S). Release of Histone H3 from chromatin was used as a control of Mnase efficiency.

(D) Half-life of endogenous chromatin-bound or soluble MDM2 was determined by quantitative immunoblotting in sh*p53*-786 cells after incubation with cycloheximide (CHX) for the indicated time.

(E) Localization of the indicated MDM2 mutants after ectopic expression in H1299 cells. Low and high exposures of the MDM2 immunoblots are shown.

See also Figure S1.

metabolism is essential for its tumor-suppressive activities (Li et al., 2012). Loss of p53 has been proposed to directly contribute to the metabolic reprogramming of cancer cells (Berkers et al., 2013; Liu et al., 2015). Besides its role in glycolysis and oxidative phosphorylation, the complexity of the metabolic network controlled by p53 is illustrated by its role in lipid and amino acid metabolism (Goldstein and Rotter, 2012; Jiang et al., 2015; Maddocks et al., 2013). However, the possibility that upstream regulators of p53 play important roles in metabolism remains poorly investigated. Here, we demonstrate that MDM2 is recruited to chromatin independently of p53 to regulate a transcriptional program involved in amino acid metabolism and the control of the redox state of cancer cells. Furthermore, we show that these previously undescribed functions of MDM2 play an important role in cancer cell proliferation and tumor growth.

RESULTS

MDM2 Is Localized in Chromatin Independently of p53

To gain insights into MDM2 oncogenic functions, we assessed MDM2 localization in a panel of cancer cell lines following biochemical fractionation of various cellular compartments. Consistent with its role as an E3 ligase, endogenous MDM2 was localized in the cyto- and nucleosoluble fractions in most of these cell lines. However, we also detected by immunoblotting a variable but significant amount of MDM2 in the chromatin-enriched fraction, ranging from 20% to 80% of the total amount of MDM2 (Figures 1A and S1A). Interestingly, the amount of chromatin-bound MDM2 did not correlate with the p53 status of these cell lines, and this recruitment was also detected in the p53-null H1299 lung cancer cell line. Consistent with the notion that MDM2 was recruited to chromatin independently of p53, small hairpin RNA (shRNA)-mediated depletion of p53 in 786.0 renal cancer cells or in MDA-MB468 breast cancer cells (hereinafter referred to as sh*p53*-786 and sh*p53*-MDA468 cells, respectively) did not alter MDM2 localization in the chromatin-enriched fraction (Figures 1B, S1B, and S1C). Digestion of DNA in the chromatin-enriched

fraction prepared from sh*p53*-786 or sh*p53*-MDA468 cells by micrococcal nuclease re-solubilized MDM2, confirming the presence of endogenous MDM2 in chromatin (Figures 1C and S1D). Next, we assessed in sh*p53*-786 cells the protein half-life of chromatin-associated and soluble MDM2 upon treatment with cycloheximide. While cyto- and nucleosoluble endogenous MDM2 protein appeared very unstable with a half-life of ~20 min, chromatin-bound MDM2 displayed increased stability with a half-life longer than 3 hr (Figure 1D).

To identify the domains involved in MDM2 recruitment to chromatin, we ectopically expressed wild-type (WT) and various MDM2 deletion mutants in H1299 cells. In line with our finding that a minor fraction of endogenous MDM2 localizes to chromatin in H1299 cells, ectopic WT MDM2 was detected in the fraction enriched in chromatin-bound proteins but mainly localized in the fraction containing soluble proteins in these cells. Strikingly, a MDM2 mutant lacking the central acidic domain (MDM2 Δ222–302, hereinafter referred to as MDM2ΔAD) was predominantly detected in the chromatin-enriched fraction (Figures 1E and S1E). Chromatin recruitment of a MDM2ΔAD mutant harboring an additional point mutation in the RING domain of MDM2 that abolishes its E3 ligase activity (MDM2ΔAD-C464A) was comparable to that of the MDM2ΔAD mutant, indicating that the E3 ligase function of MDM2 was dispensable for its recruitment to chromatin (Figures S1F and S1G).

Collectively, these data indicate that MDM2 is recruited to chromatin independently of p53 and that its central acidic domain negatively controls this recruitment.

Chromatin-Bound MDM2 Regulates an ATF-Dependent Transcriptional Program

To further characterize the roles of chromatin-bound MDM2, we then performed genome-wide chromatin immunoprecipitation (ChIP) experiments combined with next generation sequencing (ChIP-seq) using an anti-MDM2 antibody. To identify the full repertoire of p53-independent MDM2 binding sites on the genome, these ChIP-seq experiments were performed in parallel in H1299 cells transduced with a retrovirus encoding a shRNA targeting human *Mdm2* or a control shRNA and in cells expressing the chromatin-bound MDM2ΔAD mutant. The gene expression profile of H1299 cells expressing the MDM2ΔAD mutant was also compared to that of control cells by microarrays covering 35,775 human genes. Computational analyses of these datasets identified an overlay of 159 genes that were bound by MDM2 and displayed deregulated mRNA level upon increased recruitment of MDM2 to chromatin (Figure 2A; Tables S1 and S2). We confirmed in sh*p53*-MDA468 cells the direct binding of endogenous MDM2 to several of these identified MDM2 target genes by quantitative ChIP-qPCR (qChIP), including asparagine synthetase (*Asns*), phosphoserine aminotransferase 1 (*Psat1*), and Dickkopf Wnt signaling pathway inhibitor 1 (*Dkk1*) (Figure 2B). The specificity of MDM2 qChIP signal was verified in sh*p53*-MDA468 cells expressing a *Mdm2*-shRNA (Figures 2B and S2A). In H1299 cells, the MDM2-ΔAD and MDM2-ΔAD-C464A mutants were equally recruited to *Asns* and *Psat1* promoters and were both capable of increasing the mRNA levels of *Asns*, *Pck2*, and *Chac1*, indicating that MDM2-mediated regulation of its target genes occurs independently of its E3 ligase activity (Figures 2C, S2B, and S2C). Consistent with its role as a transcriptional activator, knockdown of MDM2 in H1299 cells decreased expression of this representative panel of MDM2-target genes (Figure 2C).

Bioinformatic analysis of MDM2-ChIP-seq data with two different software programs, MEME and iRegulon, revealed a statistically significant enrichment of activating transcription factor 3 and 4 (ATF3/4) motif within the chromatin fragments immunoprecipitated with MDM2 antibody, defining a subgroup of 26 out of 159 MDM2-direct target genes that were potentially co-regulated by ATFs and MDM2 ($p = 1.23E-07$) (Figures 2D and 2E). Moreover, although not performed in the same cells, we compared ATF3 and ATF4-ChIP-seq data available in ENCODE to our MDM2-ChIP-seq and microarray datasets. These comparisons identified a significant overlap between MDM2 and ATF3/4 target genes that varies from one cell type to another (Figures S2J–S2M). We experimentally confirmed in a subset of these MDM2 direct target genes (*Asns*, *Ddit4*, and *Trib3*) that they were controlled by ATF3/4, as shown by qChIP and qRT-PCR analyses performed in H1299 cells expressing ATF3/4 shRNAs (Figure S2D). To further decipher the functional relationship between chromatin-bound MDM2 and ATF3/4, we evaluated whether MDM2 and ATF4 proteins interacted using co-immunoprecipitation and GST pull-down assays. Consistent with their respective subcellular localization, endogenous ATF4 co-immunoprecipitated more efficiently with MDM2ΔAD than with WT MDM2 in H1299 cells (Figures 2F and S2H). In line with this result, in-vitro-translated ATF4 directly interacted with bacterially produced GST-MDM2ΔAD but weakly with WT GST-MDM2, as shown by GST pull-down experiments (Figure 2G). Furthermore, depletion of ATF3/4 in sh*p53*-MDA486 cells impacted the recruitment of endogenous MDM2 and of the MDM2ΔAD mutant to chromatin and to *Asns* and *Psat1* promoters (Figures 2H, 2I, and S2E–S2I).

Altogether, these results indicate that chromatin-bound MDM2 is involved in the transcriptional activation of a subset of ATF target genes independently of p53.

A Subgroup of MDM2-Target Genes Is Involved in Serine/Glycine Metabolism

Functional classification of the biological processes regulated by chromatin-bound MDM2 highlighted a potential role in amino acid metabolism and transport (Figures 3A and S3; Table S2). More specifically, MDM2 target genes were significantly enriched in genes involved in serine/glycine, glutamine, and cysteine metabolism. Since the p53 pathway was recently linked to serine and glycine metabolism (Maddocks et al., 2013), we initially focused on this class of MDM2-target genes. Serine and glycine, which are inter-converted through the activity of serine hydroxymethyltransferases (SHMTs), are two non-essential amino acids that provide anabolic precursors for the biosynthesis of macromolecules such as proteins, nucleic acids, and lipids and are also involved in redox homeostasis through the biosynthesis of glutathione. Intracellular levels of serine and glycine are maintained through uptake of exogenous pools and by de novo synthesis from the glycolytic intermediate 3-phospho glycerate (3PG) (Locasale, 2013). MDM2-responsive genes involved in serine metabolism included genes encoding the

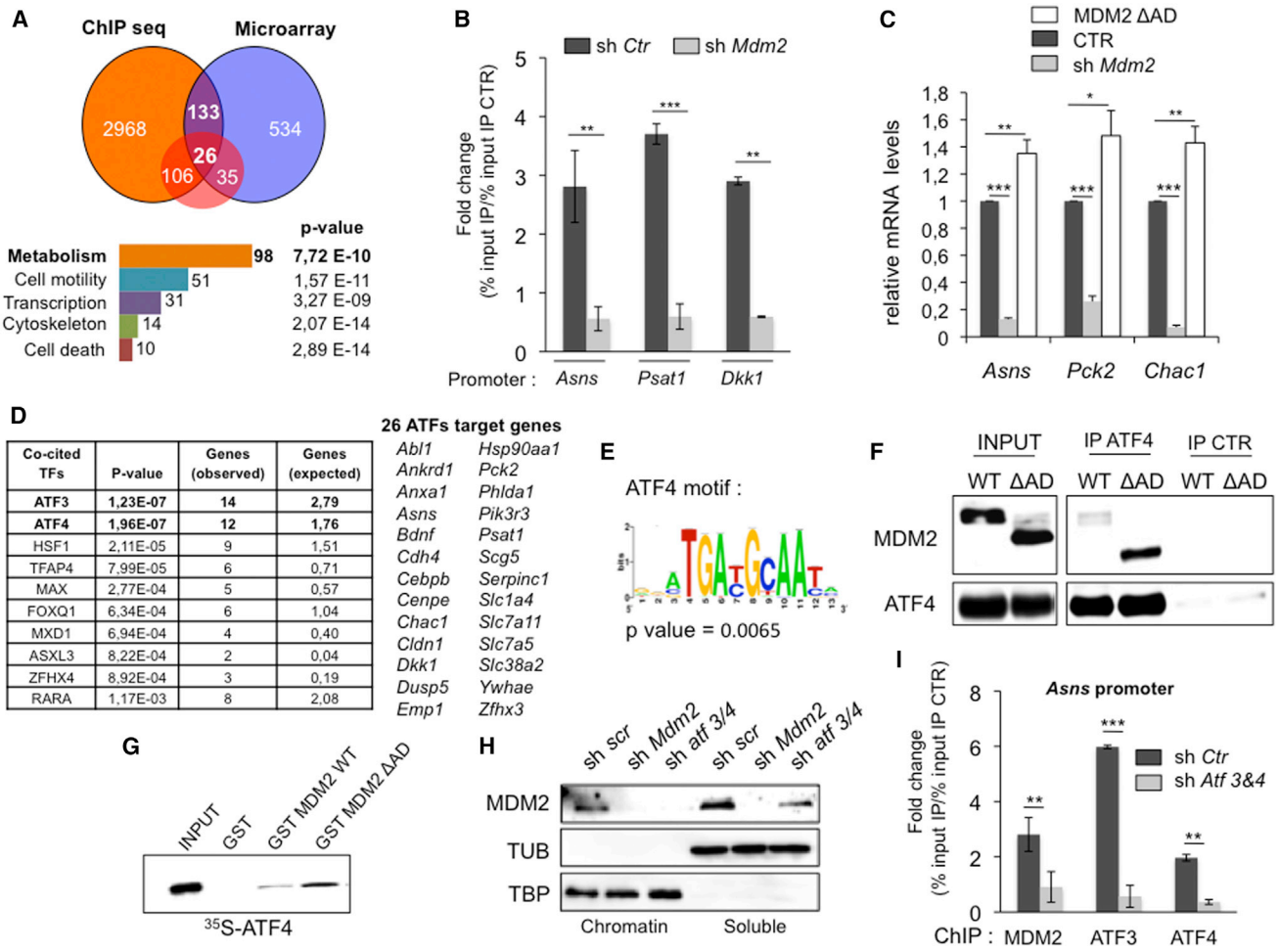

Co-cited TFs	P-value	Genes (observed)	Genes (expected)
ATF3	**1,23E-07**	**14**	**2,79**
ATF4	**1,96E-07**	**12**	**1,76**
HSF1	2,11E-05	9	1,51
TFAP4	7,99E-05	6	0,71
MAX	2,77E-04	5	0,57
FOXQ1	6,34E-04	6	1,04
MXD1	6,94E-04	4	0,40
ASXL3	8,22E-04	2	0,04
ZFHX4	8,92E-04	3	0,19
RARA	1,17E-03	8	2,08

Figure 2. Chromatin-Bound MDM2 Regulates an ATF-Dependent Transcriptional Program

(A) Venn diagram illustrating the number of MDM2 target genes identified by MDM2 ChIP-seq and gene expression profiling of H1299 cells expressing the MDM2ΔAD mutant. MDM2 binding sites were identified by ChIP-seq performed in H1299 cells using MACS with a $p = 5.10^{-5}$ by subtracting peaks identified in *Mdm2*-shRNA-treated cells to those identified in control-shRNA treated cells and cells expressing the MDM2ΔAD mutant. This gene list was intersected with the list of transcripts identified by microarray showing differential expression between cells expressing MDM2-ΔAD and control cells transfected with the empty vector ($p \leq 0.001$). The number of MDM2 target genes known to be regulated by ATFs is indicated in red in the Venn diagram. Bottom: functional annotation of this restricted list of 159 MDM2 direct target genes. The numbers of MDM2 target genes for each Gene Ontology (GO) category and the associated p value (Fisher exact test) are indicated.

(B) qChIP experiments showing the relative recruitment of endogenous MDM2 on the *Asns*, *Psat1*, and *Dkk1* loci in sh*p53*-MDA468 cells expressing control or *Mdm2*-shRNAs. Results were represented as the relative ratio between the mean value of immunoprecipitated chromatin (calculated as a percentage of the input) with MDM2 antibody and the one obtained with a control irrelevant antibody (mean ± SEM; n = 3 independent experiments).

(C) Relative mRNA levels of a representative panel of ATF target genes (*Asns*, *Pck2*, and *Chac1*) in H1299 cells, 48 hr after knockdown of MDM2 (sh*Mdm2*) (mean ± SD; n = 3), or 48 hr after expression of the MDM2ΔAD mutant (mean ± SD; n = 8). mRNA levels were determined by qRT-PCR and normalized to the corresponding control samples prepared from H1299 cells transduced with a lentivirus expressing a control-shRNA or cells transfected with an empty vector.

(D) Gene to transcription factor associations within MDM2 target genes showing significant enrichment in ATF3/4 target genes.

(E) Representation of the ATF4 motif significantly enriched in the genomic regions bound by MDM2, as determined using MEME software.

(F) Co-immunoprecipitation assays in H1999 cells showing interaction between ectopic WT MDM2 or the MDM2ΔAD mutant and endogenous ATF4 proteins. ATF4 or control immunoprecipitates were resolved on SDS-PAGE and immunoprobed with anti-MDM2 or anti-ATF4 antibodies.

(G) GST pull-down assays performed with in vitro translated [^{35}S]-methionine-radiolabeled ATF4 and GST, GST-MDM2-WT, or GST-MDM2ΔAD.

(H) Immunoblot analyses showing the level of endogenous MDM2, TBP, and TUB in sh*p53*-MDA468 cells expressing control or a combination of *Atf3*- and *Atf4*-shRNAs, in fractions enriched in chromatin-associated (chromatin) or nucleo- and cytosoluble (soluble) proteins.

(I) qChIP experiments showing the relative recruitment of MDM2, ATF3, and ATF4 on the *Asns* locus in sh*p53*-MDA468 cells expressing control shRNA or a combination of *Atf3*- and *Atf4*-shRNAs (mean ± SEM; n = 3 independent experiments).

*$p \leq 0.05$, **$p \leq 0.01$, and ***$p \leq 0.001$ indicate statistical significance of the observed differences. See also Figure S2.

A

Pathways	Metabolism	Transport
Serine / Glycine pathway	CBS, CTH, PSAT1, PSPH, PHGDH, SHMT2, ALDH1L2,GART,GOT1,GPT2, MTHFD1L, MTHFD2	SLC1A4, SERINC1
Glutamine/ Glutamate pathway	GOT1, GPT2, ASNS, BCAT1, SIRT4	SLC38A2, SLC38A1, SLC7A11, SLC7A7
Cysteine/Cystine pathway	CBS, CTH, ETHE1	SLC7A11, SLC7A9, SLC1A4
Other amino acid pathway	ADC, AMDHD1, ANXA1, ARG2, BDNF, CARS, CHAC1, CTNS, GARS,GGACT, GGTLC1, GPX1, HBB, IARS, LARS, MARS, MSRA, NEDD4L, NQO1,PSEN1, PSMB6, PYCR1, SARS, TARS, TNF, VNN1, WWP2, YWHAE	AQP1,KCNE1L, KCNMA1, KCNT2, PDZK1, SLC25A16, SLC25A20, SLC38A8, SLC3A2,SLC43A2, SLC7A5, SLCO1B1, SLCO1B3, SYT1,SLC7A1, SLC6A15

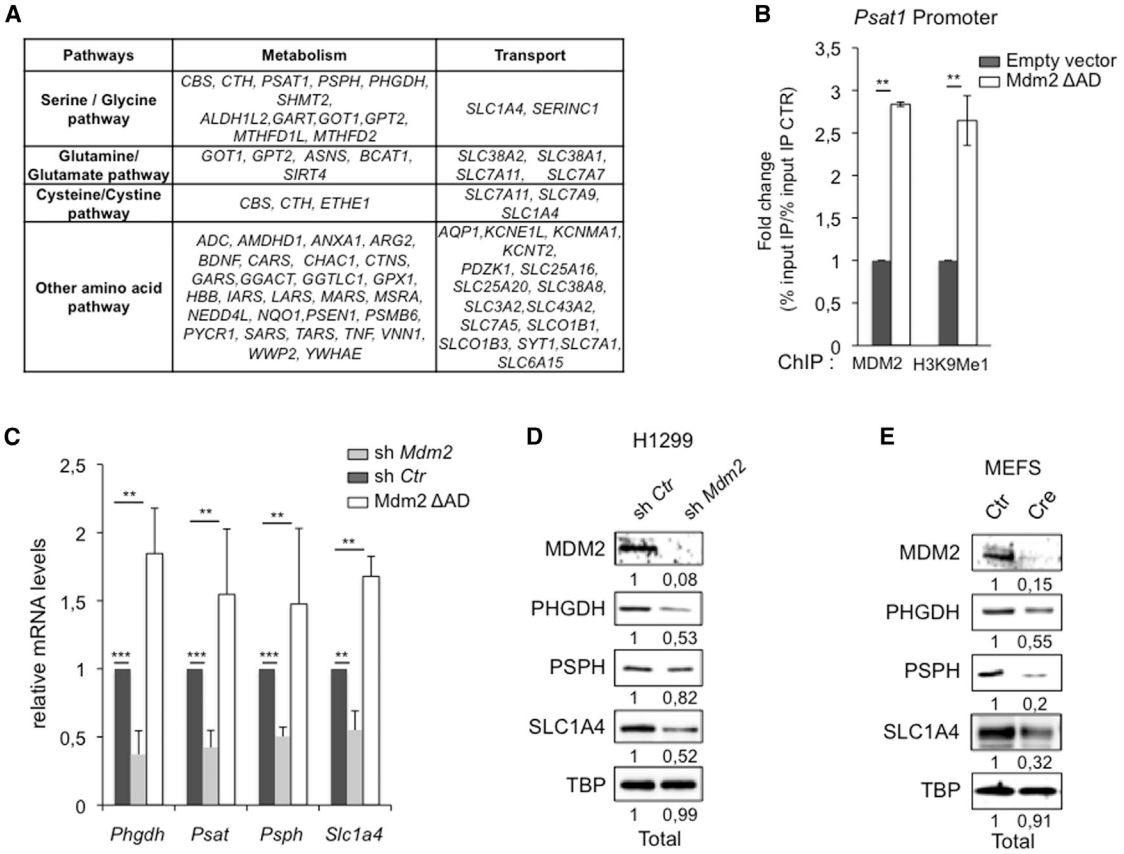

Figure 3. Chromatin-Bound MDM2 Regulates Serine Metabolism

(A) Gene set enrichment analysis (GSEA) of MDM2 responsive genes determined by gene expression profiling of H1299 cells expressing the MDM2ΔAD mutant ($p \leq 0.005$). Subclasses within the amino acid transport and metabolism category highlighted serine/glycine, glutamine/glutamate, and cysteine metabolism.

(B) qChIP experiments showing the relative amounts of chromatin-associated MDM2 and of mono-methylation of lysine 9 of histone H3 (H3K9Me1) on the *Psat1* promoter in control or H1299 cells expressing the MDM2-ΔAD mutant. Results were represented as the relative ratio between the mean value of immunoprecipitated chromatin (calculated as a percentage of the input) with the indicated antibodies and the one obtained with a control irrelevant antibody (mean ± SEM; n = 4 independent experiments).

(C) Relative mRNA levels of the MDM2-target genes *Psph*, *Psat*, *Phgdh*, and *Slc1a4* in H1299 cells 48 hr after shRNA-mediated depletion of MDM2 (sh*Mdm2*) or 48 hr after expression of the MDM2ΔAD mutant. mRNA levels were determined by qRT-PCR and normalized to the corresponding control samples prepared from H1299 cells transduced with a lentivirus expressing a control shRNA (mean ± SD; n = 3) or cells transfected with an empty vector (mean ± SD; n = 8).

(D) Protein levels of PSPH, PHGDH, and SLC1A4 were determined by quantitative immunoblotting of whole-cell extracts prepared from H1299 cells, 48 hr after transduction with a lentivirus encoding a control or Mdm2 shRNA.

(E) Protein levels of PSPH, PHGDH, and SLC1A4 in whole-cell extracts prepared from $Mdm2^{flox/flox}$; $p53^{-/-}$ MEFs 48 hr after transduction with an empty control or a Cre-encoding retrovirus.

*$p \leq 0.05$, **$p \leq 0.01$, and ***$p \leq 0.001$ indicate statistical significance of the observed differences. See also Figure S3.

3 rate limiting enzymes involved in de novo serine synthesis, phosphoglycerate dehydrogenase (*Phgdh*), *Psat1*, and phosphoserine phosphatase (*Psph*), as well as the neutral amino acid transporter *Slc1a4.* Binding of endogenous MDM2 on *Psat1* promoter was confirmed by qChIP in sh*p53*-MDA468 cells (Figure 2B). Furthermore, and consistent with reports showing that the serine-glycine synthesis pathway is regulated at the epigenetic level through methylation of histone H3 on lysine 9 (H3K9) (Ding et al., 2013; Zhao et al., 2016), the relative level of the monomethylation of H3K9 (H3K9Me1) activation mark increased upon expression of the MDM2ΔAD mutant in H1299 cells (Figure 3B). qRT-PCR analyses indicated that the mRNA levels of *Phgdh*, *Psat1*, *Psph*, and *Slc1a4* decreased in H1299 cells expressing *Mdm2*-shRNA, while they increased upon ectopic expression of the MDM2ΔAD mutant (Figure 3C). Finally, immunoblotting also showed that MDM2-deficient H1299 cells as well as *Mdm2 KO*; *p53* KO murine embryonic fibroblasts (MEFs) displayed lower amounts of PHGDH, PSPH, and SLC1A4 proteins relative to control cells (Figures 3D and 3E), confirming the role of endogenous MDM2 in the regulation of this metabolic program involved in serine/glycine metabolism.

Serine and Glycine Deprivation Regulates MDM2 Recruitment to Chromatin

Interestingly, the amount of chromatin-associated MDM2 increased when H1299 cells were shifted from a complete medium

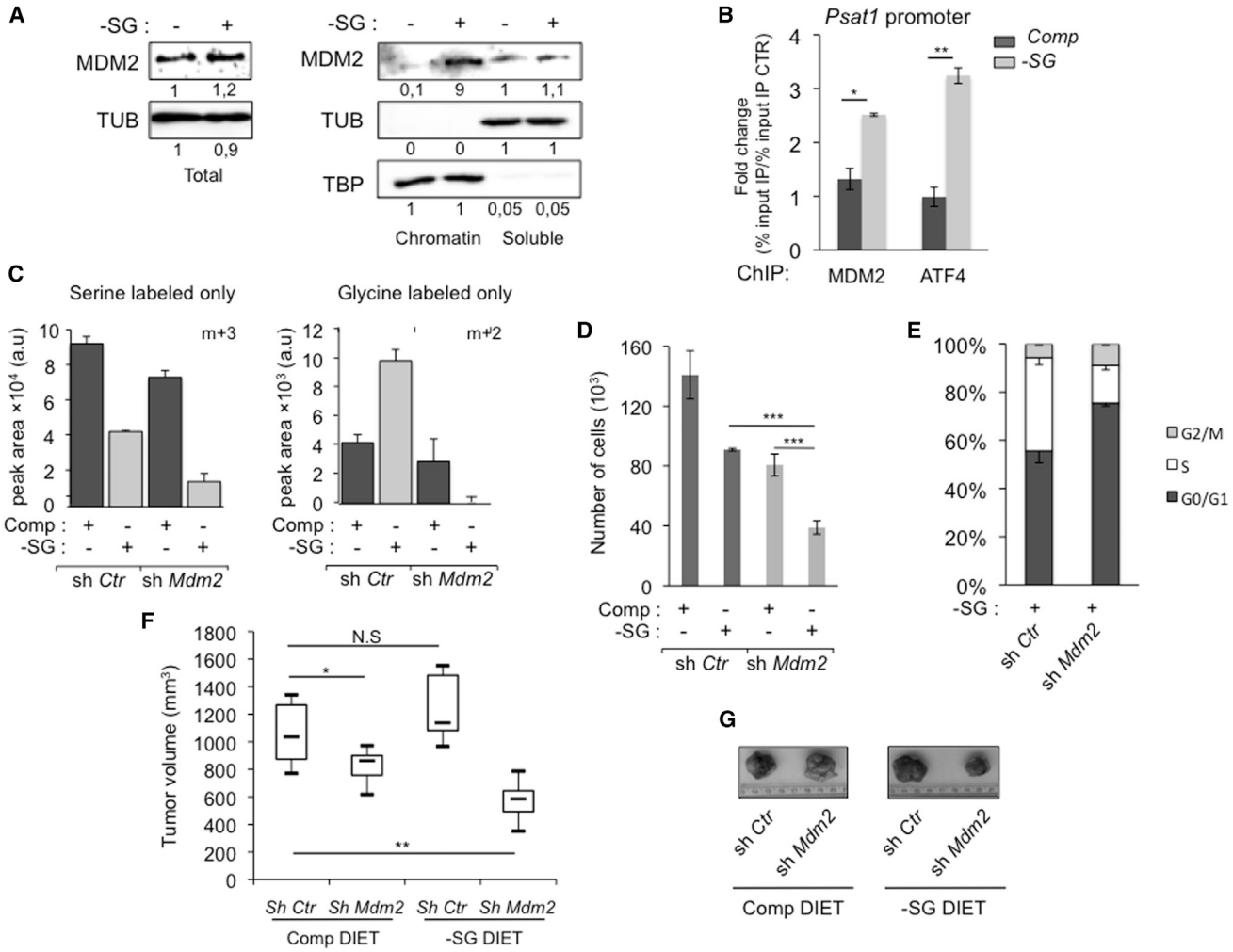

Figure 4. Serine/Glycine Deprivation Regulates MDM2 Recruitment to Chromatin

(A) Serine/glycine deprivation increases MDM2 recruitment to chromatin. Quantitative immunoblotting of MDM2, TBP, and tubulin (TUB) in whole-cell extracts (Total) or in fractions enriched in chromatin-associated (chromatin) or nucleo- and cytosoluble (soluble) proteins prepared from H1299 cells cultured in complete (Comp) or serine and glycine deprived medium (−SG). For quantification, the level of MDM2 protein detected in the soluble fraction prepared from H1299 cells cultured in Comp medium was considered as the reference level.

(B) qChIP experiments showing the relative recruitment of MDM2 and ATF4 on the *Psat1* promoter in H1299 cells cultured in Comp medium or in −SG medium. Results are represented as the relative ratio between the mean value of immunoprecipitated chromatin (calculated as a percentage of the input) with the indicated antibodies and the one obtained with a control irrelevant antibody (mean ± SEM; n = 3 independent experiments).

(C) Stable isotope tracing experiments. H1299 cells expressing a control or *Mdm2*-shRNA were cultured in Comp or −SG medium for 24 hr, in the presence of uniformly labeled [U-^{13}C]glucose for the final hour. LC-MS was used to detect the relative intracellular levels of ^{13}C-labeled (m+3) serine (left) or (m+2) glycine (right). Histobars represent the mean value of the peak area ± SD (arbitrary unit) corresponding to the serine and glycine peaks on the MS chromatogram. The experiment was performed in triplicate.

(D) Histobars represent the number of cells in control- or *Mdm2*-shRNA-treated H1299 cells cultured for 4 days in Comp medium changed every 24 hr or in −SG medium (mean ± SD; n = 3 independent experiments performed in triplicate).

(E) FACS analysis of the cell-cycle profile of H1299 cells expressing control or *Mdm2* shRNAs after 4 days of culture in −SG medium (mean ± SEM; n = 3 independent experiments).

(F) Nude mice were subcutaneously xenografted with H1299 cells stably expressing control- or *Mdm2*-shRNAs and fed with a complete or a serine- and glycine-deprived diet (−SG). Box and whisker plots represent the tumor volume (mean ± SD, n = 7 tumors per group) in each experimental group measured when one animal reached the ethical endpoint.

(G) Microphotograph of a representative tumor for each experimental group is shown.

*p ≤ 0.05, **p ≤ 0.01, and ***p ≤ 0.001 indicate statistical significance of the observed differences. NS, not significant. See also Figures S4 and S5.

to the same medium lacking serine and glycine (Figure 4A). Moreover, the level of chromatin-bound MDM2 also increased as cells progressively exhausted the exogenous pool of serine during in vitro culture, an effect that was abolished when the culture medium was replenished every 12 hr with fresh serine (Figure S4A). The recruitment of endogenous MDM2 paralleled that of ATF4

on *Asns* and *Psat1* promoters upon serine and glycine deprivation (Figures 4B and S4C). In this experimental condition, we detected a mild increase in the total level of MDM2 protein (Figure 4A) but no induction of *Mdm2* transcription (Figure S4B), suggesting that the recruitment of MDM2 to chromatin was regulated at the post-transcriptional level.

To investigate whether perturbation of this MDM2-controlled program affects the channeling of glucose-derived carbon sources into serine/glycine biosynthesis, we performed stable isotope tracing experiments. H1299 cells expressing control or *Mdm2*-shRNAs were incubated with uniformly labeled [U-^{13}C] glucose for the last hour of culture and ^{13}C-labeled intracellular metabolites were analyzed by liquid chromatography-mass spectrometry (LC-MS). When cultured in complete medium, H1299 cells expressing *Mdm2* shRNA showed a slight decrease of the total amounts (unlabeled and labeled) of intracellular serine and glycine relative to control cells (Figures S4D–S4F). Consistent with the role of MDM2 in de novo serine synthesis, the amounts of glucose-derived ^{13}C-labeled serine and glycine were further reduced when MDM2-depleted H1299 cells were cultured in serine/glycine-deprived medium (Figure 4C).

Because some cancer cells are highly dependent on serine/glycine metabolism for proliferation (Jain et al., 2012; Locasale et al., 2011; Possemato et al., 2011), we hypothesized that interfering with this MDM2-regulated metabolic program would impact the growth of serine/glycine-deprived cells. Accordingly, the growth defect of MDM2-depleted H1299 cells was enhanced when these cells were cultured in serine/glycine-deprived medium (Figures 4D, S5A, and S5B). A comparable effect was observed in HCT116 *p53*KO and sh*p53*-786 cells (Figures S5C–S5F). Fluorescence-activated cell sorting (FACS) analysis of the cell-cycle profile of MDM2-deficient H1299 cells indicated that these cells underwent a potent arrest in the G1 phase of the cell cycle when cultured in a serine/glycine-deprived medium (Figure 4E). Next, we evaluated the impact of MDM2-mediated control of serine/glycine metabolism on tumor growth in vivo. H1299 cells stably expressing control or *Mdm2* shRNAs were subcutaneously injected in nude mice that were fed with a normal diet or a serine/glycine deprived diet of equivalent calorific value and equal content in total amino acids. Strikingly, the lack of diet-derived serine and glycine impaired the tumorigenic potential of MDM2-depleted H1299 cells, with no or little impact on that of control H1299 cells (Figures 4F, 4G, and S5G–S5I).

Thus, these data indicate that serine/glycine deprivation triggers MDM2 recruitment to chromatin to activate a transcriptional program that sustains serine synthesis and tumor growth.

MDM2 Regulates Redox Homeostasis in Cancer Cells Independently of p53

Notably, genes implicated in redox homeostasis were also statistically overrepresented among MDM2 target genes. This category contained genes controlling glutathione (GSH) synthesis and recycling, as well as genes involved in anti-oxidant defenses (Figure 5A; Table S2). The mRNA levels of genes of this category decreased upon MDM2-depletion in H1299, as exemplified by glutathione peroxidase 1 (*Gpx1*), NAD(P)H dehydrogenase quinone 1 (*Nqo1*), and pyrroline-5-carboxylate reductase 1 (*Pycr1*) (Figure 5B).

To study the role of MDM2 in redox homeostasis, we investigated how chromatin-bound MDM2 impinged on GSH metabolism, on the NAD$^+$/NADH ratio, and on the level of reactive oxygen species (ROS). In H1299 cells cultured in complete medium, the level of reduced GSH increased moderately in MDM2-depleted cells, whereas it decreased in cells expressing the MDM2ΔAD mutant. The amount of oxidized glutathione (GSSG) strongly decreased in MDM2-depleted H1299 cells (Figure 5C), suggesting that MDM2 deficiency did not impair GSH synthesis in those fed conditions but rather impacted on the GSH-GSSG cycle. Then, we evaluated whether MDM2 also influenced the NAD$^+$/NADH ratio. In H1299 cells, the NAD$^+$/NADH ratio dropped upon MDM2 depletion (Figure 5D). To further illustrate the role of MDM2 on redox homeostasis, we measured the intracellular ROS levels by flow cytometry using the CM-H2DCFDA probe and by immunoblot detection of carbonyl groups introduced into proteins by oxidative reactions (Oxyblot). MDM2 depletion resulted in increased ROS levels, whereas ectopic expression of the MDM2ΔAD mutant reduced ROS levels in H1299 cells (Figure 5E). The increased ROS levels in MDM2-depleted H1299 cells were partly rescued upon ectopic expression of a shRNA-resistant WT-MDM2 protein (Figure S6F). Moreover, ROS levels in H1299 cells expressing the MDM2ΔAD and the MDM2ΔAD-C464A mutants were comparable (data not shown), indicating that MDM2 function in redox homeostasis was independent of its E3 ligase activity. Protein carbonylation correlated with these changes in ROS levels. Thus, MDM2-depleted cells displayed uncompensated oxidative damages to proteins, whereas cells expressing the MDM2-ΔAD mutant exhibited the opposite profile (Figure 5F).

Next, we evaluated whether the role of MDM2 in redox homeostasis influenced cell growth. Consistent with their imbalanced redox status, we found that the ROS scavenger *N*-acetylcysteine (NAC) partly rescued the growth of MDM2-depleted H1299 cells in vitro as well as their tumorigenic potential in vivo under serine/glycine-deprived conditions (Figures 5G, 5H, S6A, and S6B). These data indicated that increased ROS production partly contributed to the growth defect of MDM2-depleted H1299 cells. We also addressed the impact of the altered NAD$^+$/NADH ratio on the proliferation rate of these cells by providing an exogenous source of pyruvate to MDM2-depleted H1299 cells. Pyruvate has several metabolic fates, both in the mitochondria and in the cytosol. Cytosolic pyruvate can generate NAD$^+$ through the lactate dehydrogenase (LDH)-driven reaction (Sullivan et al., 2015). Strikingly, pyruvate addition potently rescued the growth of MDM2-depleted H1299 cells under serine/glycine deprivation (Figures 5I and S6D). We excluded that pyruvate restored cell growth of MDM2-depleted cells by fueling mitochondria, since a comparable rescue was observed upon concomitant addition of a pharmacological inhibitor of the mitochondrial pyruvate transporter MPC1 (Halestrap, 1975) (Figure S6C). Addition in the culture medium of alpha-ketobutyrate (AKB), an electron acceptor that can act as an alternative substrate for LDH, also partly restored the proliferation of MDM2-depleted cells under serine/glycine deprivation (Figure S6E). Hence, these data demonstrate that the p53-independent role of MDM2 on redox homeostasis is important for cell growth of cancer cells.

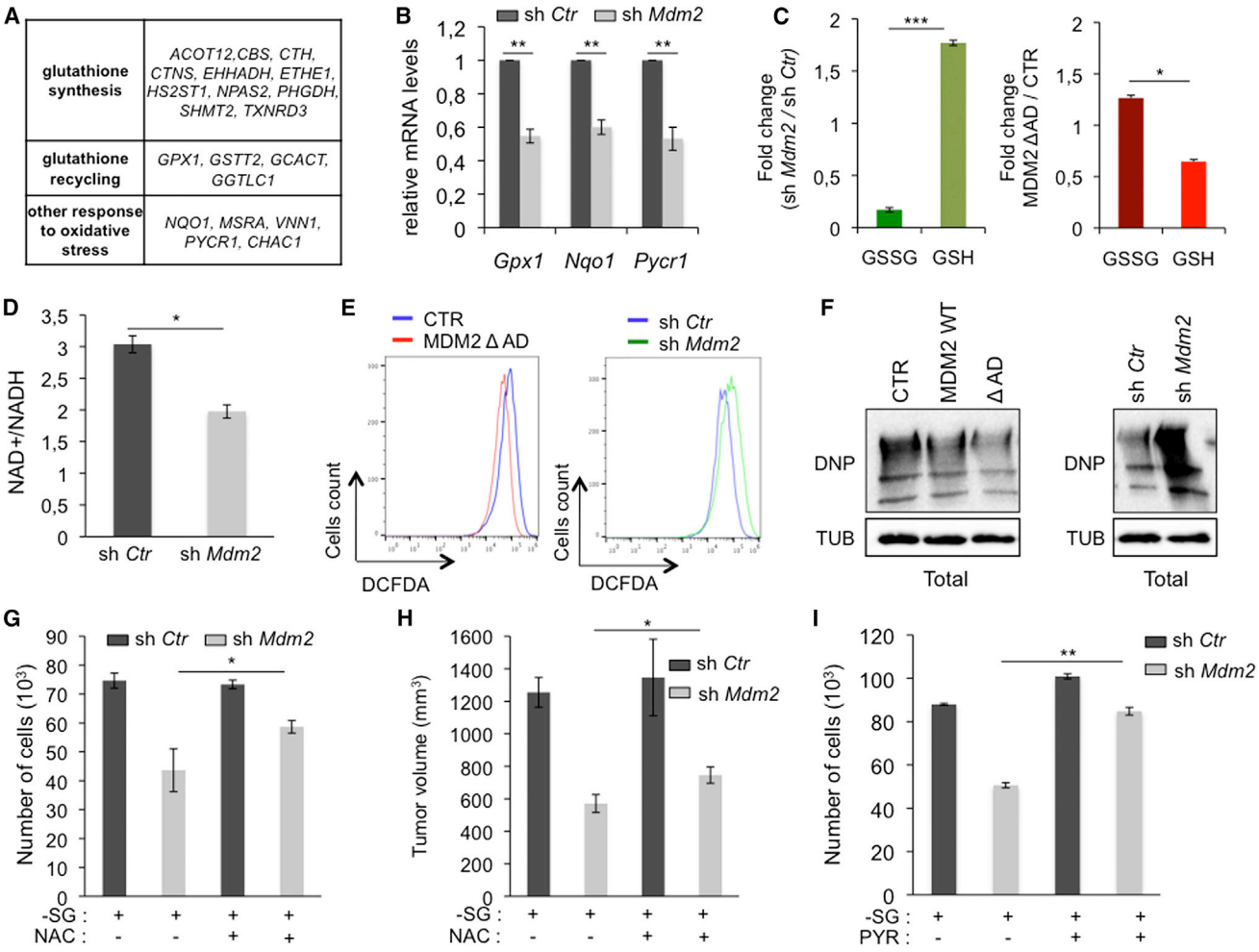

Figure 5. MDM2 Regulates Redox Homeostasis

(A) Gene list of MDM2 target genes implicated in glutathione metabolism and oxidative stress determined by gene expression profiling of H1299 cells expressing the MDM2ΔAD mutant ($p \leq 0.005$).

(B) qRT-PCR analysis of *Gpx1*, *Nqo1*, and *Pycr1* mRNA levels in H1299 cells expressing control or *Mdm2* shRNAs cultured in complete medium (mean ± SD of n = 3 independent experiments).

(C) Relative levels of oxidized (GSSG) and reduced (GSH) glutathione in H1299 cells expressing control or *Mdm2*-shRNAs (left) or in H1299 cells transfected with an empty vector or expressing the MDM2ΔAD mutant (right) (mean ± SD, n = 3).

(D) NAD^+/NADH ratio in H1299 cells expressing control- or *Mdm2*-shRNAs.

(E) Left: ROS levels in H1299 cells transfected with an empty vector or with the MDM2ΔAD mutant determined by flow cytometry using the fluorophore dichlorodihydrofluorescein diacetate (DCFDA) probe. Right: ROS levels in H1299 cells expressing control or *Mdm2*-shRNAs. Data are representative of four independent experiments.

(F) Immunoblot analyses of the levels of protein carbonylation (DNP) in control H1299 cells or cells expressing ectopic WT MDM2 or the MDM2ΔAD mutant (left) or in H1299 cells expressing control or *Mdm2*-shRNAs (right panel).

(G) The ROS scavenger NAC partly rescues the growth of MDM2-deficient H1299 cells cultured in serine/glycine-deprived medium (−SG). Histobars represent the number of cells after 4 days of culture in the indicated conditions (mean ± SD; n = 3 independent experiments performed in triplicates).

(H) NAC treatment partly rescues tumor growth of MDM2-deficient H1299 cells in nude mice fed with a serine- and glycine-deprived (−SG) diet. Box and whisker plots representing the tumor volume (mean ± SD, n = 7 tumors per group) in each experimental group measured when the first animal reached the ethical endpoint.

(I) Pyruvate (PYR) partly rescues the growth of MDM2-deficient H1299 cells cultured in −SG medium. Histobars represent the number of cells after 4 days of culture in the indicated conditions (mean ± SD; n = 3 independent experiments performed in triplicate).

*$p \leq 0.05$, **$p \leq 0.01$, and ***$p \leq 0.001$ indicate statistical significance of the observed differences. See also Figure S6.

PKM2 and Oxidative Stress Control MDM2 Recruitment to Chromatin

In order to gain insights into the molecular mechanisms underlying MDM2 recruitment to DNA, we monitored MDM2 localization in p53-deficient H1299, HCT116 *p53*KO cells and $p53^{-/-}$ MEFs exposed to various stress conditions. Addition of pro-oxidant molecules including menadione or hydrogen peroxide (H_2O_2), but not genotoxic stress induced by 5-fluoro-uracil (5FU), UV,

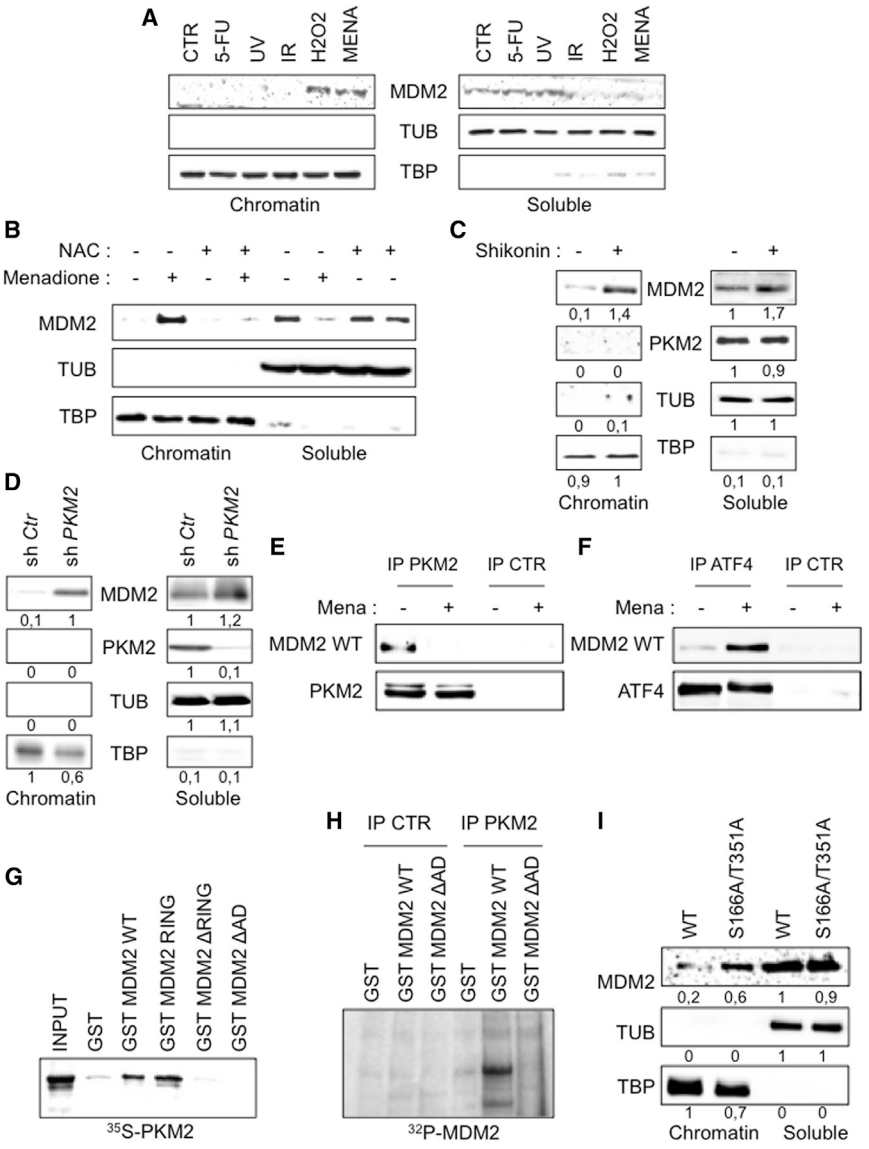

Figure 6. PKM2 and Oxidative Stress Control MDM2 Recruitment to Chromatin

(A) Quantitative immunoblotting of MDM2, TBP, and tubulin (TUB) in fractions enriched in chromatin-associated (chromatin) or nucleo- and cytosoluble (soluble) proteins prepared from H1299 cells after DNA damage (5-fluorouracil [5FU], UV, or ionizing radiation [IR]) or after treatment with pro-oxidants (H_2O_2, menadione [MENA]).

(B) The levels of chromatin-bound or soluble endogenous MDM2 were determined in H1299 cells upon menadione-induced oxidative stress in the presence or absence of NAC.

(C and D) PKM2 activity influences MDM2 recruitment to chromatin. The level of chromatin-bound MDM2 was evaluated by quantitative immunoblotting in mock-treated H1299 cells or in cells treated with the pharmacological PKM2 inhibitor shikonin (C) or in cells expressing *Pkm2* shRNA (D). For quantification, the level of MDM2 protein detected in the soluble fraction prepared from control H1299 cells was considered as the reference level.

(E and F) Protein-protein interactions between ectopic WT-MDM2 and endogenous ATF4 or endogenous PKM2 under oxidative stress were evaluated in H1299 cells by co-immunoprecipitation assays. 48 hr after transfection, H1999 cells expressing WT-MDM2 were treated for 1 hr with menadione (MENA) before being processed for immunoprecipitation using anti-PKM2 (E) or anti-ATF4 (F) antibodies. Immunoprecipitates were analyzed by immunoblotting with anti-MDM2, anti-PKM2, or anti-ATF4 antibodies.

(G) GST pull-down assays performed with in-vitro-translated [^{35}S]-methionine-radiolabeled PKM2 and GST or GST-tagged WT-MDM2, MDM2ΔAD, MDM2ΔRING, and the RING domain of MDM2 alone (MDM2 RING).

(H) In vitro kinase assays performed with a control immunoprecipitation (IP CTR) or immunoprecipitated PKM2 (IP PKM2) from H1299 cells and purified recombinant GST-WT-MDM2 or GST-MDM2ΔAD proteins as a substrate in the presence of [^{32}P]-ATP.

(I) Alanine substitution of the two major PKM2-dependent phosphorylation sites (residues S166 and T351) identified by MS-MS phosphopeptide mapping increases MDM2 recruitment to chromatin. Levels of chromatin-bound or soluble WT-MDM2 or MDM2-S166A/T351A were determined by quantitative immunoblotting in H1299 cells. Experimental conditions were adjusted to ensure equal expression of both proteins that display different stability at the time chromatin fractionation was performed. For quantification, the level of MDM2 protein detected in the soluble fraction prepared from H1299 cells expressing WT-MDM2 was considered as the reference level.

See also Figure S7.

or ionizing radiation, relocalized cyto/nucleosoluble MDM2 to chromatin in H1299 cells (Figures 6A, S7A, and S7B). In H1299 cells, recruitment of endogenous MDM2 to chromatin occurred as early as 5 min after incubation with menadione and was abolished in the presence of NAC (Figure 6B). A previous report showed that the activity of the M2 isoform of pyruvate kinase (PKM2), a key metabolic enzyme that converts phosphoenolpyruvate into pyruvate, is inhibited by ROS. ROS-mediated inhibition of PKM2 activity increases anti-oxidant defenses by promoting the redirection of glycolytic intermediates toward the serine biosynthetic and the pentose phosphate pathways (Anastasiou et al., 2011). Moreover, serine is an allosteric activator of PKM2 (Chaneton et al., 2012). These data prompted us to evaluate whether PKM2 is involved in the control of MDM2 recruitment to chromatin. Consistent with this hypothesis, we found that pharmacological inhibition of PKM2 activity by shikonin in H1299 cells, or knockdown of PKM2, relocalized endogenous MDM2 in chromatin (Figures 6C and 6D). Shikonin-mediated recruitment of MDM2 to chromatin was abolished in H1299 cells expressing shRNAs targeting ATF3 and ATF4 (Figure S7C), linking PKM2 activity and MDM2-mediated control of ATF target genes.

To further characterize the mechanisms by which PKM2 regulates MDM2, we performed co-immunoprecipitation, pull-down

and in vitro phosphorylation assays. Ectopic WT-MDM2 co-immunoprecipitated with endogenous PKM2 in protein extracts prepared from H1299 cells cultured in absence of menadione (Figure 6E). Strikingly, the PKM2-MDM2 interaction was lost upon menadione-induced oxidative stress that instead promoted the association of WT-MDM2 with endogenous ATF4 (Figures 6E and 6F). MDM2 and PKM2 interacted directly, as shown by GST pull-down assays, and this protein-protein interaction required both the RING-E3 ligase and the acidic domains of MDM2 (Figure 6G). Furthermore, GST-WT MDM2, but not GST-MDM2ΔAD, was efficiently phosphorylated in vitro by a PKM2 complex that was immunoprecipitated from H1299 cells (Figure 6H). Pre-incubation of H1299 cells with shikonin prevented the phosphorylation of MDM2 by immunoprecipitated PKM2 (Figure S7D). Next, we analyzed MDM2 phosphopeptides by mass spectrometry and identified serine 166 (S166) and threonine 351 (T351) of MDM2 to be phosphorylated in vitro by this immunoprecipitated PKM2 complex (Figure S7E). A MDM2 mutant in which S166 and T351 were mutated to non-phosphorylatable alanine residues (MDM2-S166A/T351A) displayed increased stability and increased localization in chromatin relative to WT-MDM2 (Figure 6I; data not shown), confirming the inhibitory role of PKM2-dependent phosphorylation on MDM2 recruitment to chromatin.

Altogether, these data show that MDM2 is involved in a regulatory loop in which oxidative stress and PKM2 control MDM2-recruitment to chromatin to sustain an anti-oxidant response.

DISCUSSION

Metabolic rewiring is considered a hallmark of malignant transformation, and multiple oncogenes and tumor suppressors control various metabolic pathways (Boroughs and DeBerardinis, 2015). Among those, the p53 protein is recognized as a central regulator of metabolism, but the role of other components of the p53 pathway in metabolism has been so far poorly investigated. Here, we show that MDM2, a bona fide oncogene and essential component of this pathway, regulates serine metabolism and redox homeostasis independently of p53. Our data, together with a previous report showing that MDM2 can ubiquitylate and directly control dihydrofolate reductase (DHFR) (Maguire et al., 2008), underline a previously underestimated function of MDM2 in metabolism.

Serine/glycine metabolism supports the growth of cancer cells by contributing to their anabolic demands and epigenome as well as by regulating their redox state (Locasale, 2013). Strikingly, we found that MDM2 operates independently of p53 to control serine/glycine metabolism and sustain cancer growth in conditions of serine and glycine deprivation. Our results indicate that interfering with MDM2 functions when cancer cells face depleted pools of exogenous serine and glycine compromises their proliferative capacities and tumorigenic potential. These phenotypes result, at least in part, from perturbations of their redox state, likely through several mechanisms impinging on GSH metabolism, the NAD^+/NADH ratio, and ROS levels. Consistent with this notion, addition of the ROS scavenger NAC or exogenous pyruvate partly rescued the growth of MDM2-depleted cells under serine and glycine deprivation. However, given the central role of serine/glycine metabolism in various anabolic pathways, the metabolic consequences of MDM2 depletion under serine and glycine deprivation are likely to be broader than the observed perturbation of the redox state of these cells. The recent findings that serine metabolism plays an essential role in one carbon cycle for the generation of S-adenosyl-methionine (SAM) (Maddocks et al., 2016), a major methyl-donor co-factor involved in histone and DNA/RNA methylation, raise interesting questions regarding the potential links between MDM2 deregulation and epigenetic alterations that commonly occur during cancer progression. Our pan-genome analysis of MDM2-target genes suggests that MDM2 functions in cancer cell metabolism extend beyond serine/glycine metabolism and may also control cysteine and glutamine levels.

Our data support the notion that MDM2 plays a central role in the metabolic network regulated by PKM2. Indeed, MDM2 is efficiently recruited to chromatin in cells exhibiting low PKM2 activity, as well as in two experimental conditions, oxidative stress and serine deprivation, that alter PKM2 activity. Furthermore, we identified Ser166 and Thr351 to be phosphorylated in a PKM2-dependent manner. Nevertheless, our results obtained with recombinant proteins, as well as those from a recent study showing that PKM2 lacks protein kinase activity (Hosios et al., 2015), do not support the notion that MDM2 is a direct target of PKM2 but rather of a yet-unidentified kinase that associates with PKM2. Interestingly, phosphorylation of MDM2 on Ser166 by AKT was previously shown to control its subcellular localization (Mayo and Donner, 2001), and Thr351 was recently identified as a minor phosphorylation site of the mitotic checkpoint kinase MPS1 in response to oxidative stress (Yu et al., 2016). Here, we show the inhibitory role of these phosphorylation sites on MDM2 recruitment to chromatin. Our data also identified the central acidic domain as an inhibitory domain limiting MDM2 recruitment to chromatin. A recent study suggested that this domain plays a conformational role for the protein that is required for MDM2-E3 ligase activity through intramolecular binding with the RING domain (Cheng et al., 2014). Consistent with these data, we found that MDM2-E3 ligase activity is dispensable for its recruitment to chromatin, regulation of its target genes, and control of ROS levels.

Several studies have underlined the role of ATF transcription factors in the regulation of a subset of MDM2 target genes, including those implicated in serine biosynthesis (DeNicola et al., 2015; Ye et al., 2012). Our data clearly indicate that MDM2-recruitement to chromatin triggered by oxidative stress or low PKM2 activity is independent of p53 but involves the ATF3/4 transcription factors. These results, together with those showing that MDM2-mediated ubiquitylation of ATF3 controls its stability (Mo et al., 2010) and that ATF3 enhances transactivation of p53 target genes, including *Mdm2* (Yan et al., 2005), illustrate a complex interplay between the p53 pathway and ATF family members. Interestingly, the G9A methyltransferase and the histone lysine demethylase KDM4C have been linked to the transcriptional regulation of serine synthesis genes (Ding et al., 2013; Zhao et al., 2016). Further studies are warranted to evaluate whether these epigenetic regulators are recruited together with MDM2 and ATF4 to control the transcription of these genes.

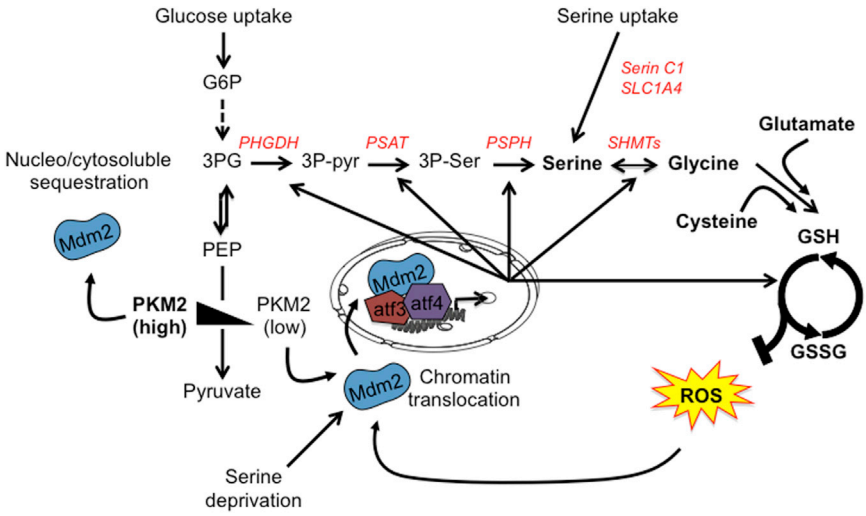

Figure 7. MDM2 Is a Key Regulator of Metabolism to Sustain Cellular Anti-oxidant Defenses

Schematic model showing how the recruitment of MDM2 to chromatin contributes to serine/glycine and glutathione metabolism. MDM2 recruitment to ATF3/4-target genes is increased upon serine deprivation, oxidative stress, or low PKM2 activity to sustain the expression of genes involved in serine/glycine and glutathione metabolism. G6P, glucose 6-phosphate; PEP, phosphoenolpyruvate; 3PG, 3-phosphoglycerate; 3P-Pyr, 3-phosphohydroxypyruvate; 3P-Ser, 3-phosphoserine; GSH, glutathione.

In line with this hypothesis, MDM2 recruitment to its target genes correlated with increased histone H3 monomethylation on lysine 9, an epigenetic mark regulated by KDM4C and G9A. Altogether, these data highlight a previously unsuspected network involving PKM2, MDM2, and ATFs in the regulation of a transcriptional program involved in serine metabolism and redox homeostasis (Figure 7).

A previous study pinpointed that p53-mutated cells are hypersensitive to serine and glycine deprivation (Maddocks et al., 2013). The potential connections of these observations with our findings showing that MDM2 regulates serine metabolism may reflect the well-described role of p53 on *Mdm2* transcription and the documented downregulation of MDM2 in many p53 null cells (Barak et al., 1993; Wu and Levine, 1997). However, other reports showing that p53 directly represses several MDM2 target genes identified in our study, including *Phgdh* (Ou et al., 2015) and *Slc7A11* (Jiang et al., 2015), illustrate the complex roles of the p53 pathway in these metabolic pathways. Finally, the clinical implications of our findings are underlined by bioinformatic analyses showing the significance of the expression level of genes involved in serine metabolism, including *Phgdh* and *Shmt2*, to predict breast and lung cancer patient survival (Antonov et al., 2014; DeNicola et al., 2015). Our data showing that MDM2 controls cancer cell metabolism pave the way for therapeutic strategies targeting these unexpected functions of this commonly deregulated oncogene, in particular in cancers harboring MDM2 overexpression.

EXPERIMENTAL PROCEDURES

Subcellular Fractionation and Micrococcal Nuclease Treatment

The protocol for subcellular fractionation was adapted from a previously described method, as described in Supplemental Experimental Procedures (Wysocka et al., 2001). Pooled cyto- and nucleosoluble proteins and chromatin-associated proteins were then analyzed in parallel by immunoblotting.

ChIP-Seq Analysis

Next-generation sequencing was performed upon ChIP with anti-MDM2 N20 antibody in H1299 cells expressing a shRNA targeting *Mdm2* and in cells overexpressing MDM2-ΔAD mutant. Samples were processed in vitro to generate a library of short inserts of ~250 bp. The library was sequenced on an Illumina HiSeq 2000 platform. Reads were trimmed at 50 bp for single-read runs using the "forward" sequencing primer. The data were then processed using bioinformatics tools to extract biologically useful information. Briefly, alignment with human genome Hg19 was done with Bowtie for Illumina and Pics calling with model-based analysis of ChIP-seq (MACS) 1.0.1. Functional gene annotation was performed using Great, and GO term analysis was performed with Genomatix.

Statistical Analysis

Data are expressed as mean ± SD. The results were analyzed by a Student's t test, and p values less than 0.05 were considered to be statistically significant (*$p < 0.05$, $0.01 <$ **$p < 0.001$, and ***$p < 0.001$).

Xenografts

Bilateral subcutaneous injections of H1299 cells were carried out on 8-week-old CD-1-Foxn1nu mice (Charles River) as described in the Supplemental Information. Mice were housed in a pathogen free barrier facility in accordance with the regional ethic committee for animal warfare (n°CEEA-LR- 12067).

ACCESSION NUMBERS

The accession number for the complete transcriptomic profiles reported in this paper is GEO: GSE64439.

SUPPLEMENTAL INFORMATION

Supplemental Information includes Supplemental Experimental Procedures, seven figures, and two tables and can be found with this article online at http://dx.doi.org/10.1016/j.molcel.2016.04.033.

AUTHOR CONTRIBUTIONS

R.R., L.L., and L.K.L. designed the studies, interpreted the data, and wrote the manuscript; R.R., L.K.L., E.S., E.B., F.S., M.Y.C., T.L., M.H., F.B., and G.A. performed the experiments; L.K.L. and F.R. performed the bioinformatic analyses; R.R., L.K.L., C.V., and I.A.-A. contributed to the in vivo experiments; and J.C.M., J.C.P., P.T., and J.E.S. assisted with data interpretation.

ACKNOWLEDGMENTS

The authors thank A. Jochemsen and Y. Haupt for *Mdm2* constructs, O. Maddock and K. Vousden for stable isotope labeling experiments, M. Selak and M. Lacroix for input and critical reading of the manuscript, and members of the histology and animal facilities of Montpellier BioCampus for technical assistance. This research was supported by grants from the Institut National du Cancer (INCa), the Ligue contre le Cancer (Equipe labelisée 2016), and the

INSERM-Avenir program. R.R. was supported by a fellowship from the French Ministry of Research and the ARC Foundation. G.A. was supported by the Région Languedoc Roussillon and the University of Montpellier.

Received: October 19, 2015
Revised: March 7, 2016
Accepted: April 27, 2016
Published: June 2, 2016

REFERENCES

Anastasiou, D., Poulogiannis, G., Asara, J.M., Boxer, M.B., Jiang, J.-K., Shen, M., Bellinger, G., Sasaki, A.T., Locasale, J.W., Auld, D.S., et al. (2011). Inhibition of pyruvate kinase M2 by reactive oxygen species contributes to cellular antioxidant responses. Science *334*, 1278–1283.

Antonov, A., Agostini, M., Morello, M., Minieri, M., Melino, G., and Amelio, I. (2014). Bioinformatics analysis of the serine and glycine pathway in cancer cells. Oncotarget *5*, 11004–11013.

Barak, Y., Juven, T., Haffner, R., and Oren, M. (1993). mdm2 expression is induced by wild type p53 activity. EMBO J. *12*, 461–468.

Berkers, C.R., Maddocks, O.D.K., Cheung, E.C., Mor, I., and Vousden, K.H. (2013). Metabolic regulation by p53 family members. Cell Metab. *18*, 617–633.

Biderman, L., Manley, J.L., and Prives, C. (2012). Mdm2 and MdmX as regulators of gene expression. Genes Cancer *3*, 264–273.

Bohlman, S., and Manfredi, J.J. (2014). p53-independent effects of Mdm2. Subcell. Biochem. *85*, 235–246.

Boroughs, L.K., and DeBerardinis, R.J. (2015). Metabolic pathways promoting cancer cell survival and growth. Nat. Cell Biol. *17*, 351–359.

Chaneton, B., Hillmann, P., Zheng, L., Martin, A.C.L., Maddocks, O.D.K., Chokkathukalam, A., Coyle, J.E., Jankevics, A., Holding, F.P., Vousden, K.H., et al. (2012). Serine is a natural ligand and allosteric activator of pyruvate kinase M2. Nature *491*, 458–462.

Cheng, Q., Song, T., Chen, L., and Chen, J. (2014). Autoactivation of the MDM2 E3 ligase by intramolecular interaction. Mol. Cell. Biol. *34*, 2800–2810.

Cordon-Cardo, C., Latres, E., Drobnjak, M., Oliva, M.R., Pollack, D., Woodruff, J.M., Marechal, V., Chen, J., Brennan, M.F., and Levine, A.J. (1994). Molecular abnormalities of mdm2 and p53 genes in adult soft tissue sarcomas. Cancer Res. *54*, 794–799.

DeNicola, G.M., Chen, P.-H., Mullarky, E., Sudderth, J.A., Hu, Z., Wu, D., Tang, H., Xie, Y., Asara, J.M., Huffman, K.E., et al. (2015). NRF2 regulates serine biosynthesis in non-small cell lung cancer. Nat. Genet. *47*, 1475–1481.

Ding, J., Li, T., Wang, X., Zhao, E., Choi, J.-H., Yang, L., Zha, Y., Dong, Z., Huang, S., Asara, J.M., et al. (2013). The histone H3 methyltransferase G9A epigenetically activates the serine-glycine synthesis pathway to sustain cancer cell survival and proliferation. Cell Metab. *18*, 896–907.

Goldstein, I., and Rotter, V. (2012). Regulation of lipid metabolism by p53 - fighting two villains with one sword. Trends Endocrinol. Metab. *23*, 567–575.

Halestrap, A.P. (1975). The mitochondrial pyruvate carrier. Kinetics and specificity for substrates and inhibitors. Biochem. J. *148*, 85–96.

Hosios, A.M., Fiske, B.P., Gui, D.Y., and Vander Heiden, M.G. (2015). Lack of Evidence for PKM2 Protein Kinase Activity. Mol. Cell *59*, 850–857.

Jain, M., Nilsson, R., Sharma, S., Madhusudhan, N., Kitami, T., Souza, A.L., Kafri, R., Kirschner, M.W., Clish, C.B., and Mootha, V.K. (2012). Metabolite profiling identifies a key role for glycine in rapid cancer cell proliferation. Science *336*, 1040–1044.

Jiang, L., Kon, N., Li, T., Wang, S.J., Su, T., Hibshoosh, H., Baer, R., and Gu, W. (2015). Ferroptosis as a p53-mediated activity during tumour suppression. Nature *520*, 57–62.

Jones, S.N., Roe, A.E., Donehower, L.A., and Bradley, A. (1995). Rescue of embryonic lethality in Mdm2-deficient mice by absence of p53. Nature *378*, 206–208.

Jones, S.N., Hancock, A.R., Vogel, H., Donehower, L.A., and Bradley, A. (1998). Overexpression of Mdm2 in mice reveals a p53-independent role for Mdm2 in tumorigenesis. Proc. Natl. Acad. Sci. USA *95*, 15608–15612.

Khoo, K.H., Verma, C.S., and Lane, D.P. (2014). Drugging the p53 pathway: understanding the route to clinical efficacy. Nat. Rev. Drug Discov. *13*, 217–236.

Li, Q., and Lozano, G. (2013). Molecular pathways: targeting Mdm2 and Mdm4 in cancer therapy. Clin. Cancer Res. *19*, 34–41.

Li, T., Kon, N., Jiang, L., Tan, M., Ludwig, T., Zhao, Y., Baer, R., and Gu, W. (2012). Tumor suppression in the absence of p53-mediated cell-cycle arrest, apoptosis, and senescence. Cell *149*, 1269–1283.

Liu, J., Zhang, C., Hu, W., and Feng, Z. (2015). Tumor suppressor p53 and its mutants in cancer metabolism. Cancer Lett. *356* (2 Pt A), 197–203.

Locasale, J.W. (2013). Serine, glycine and one-carbon units: cancer metabolism in full circle. Nat. Rev. Cancer *13*, 572–583.

Locasale, J.W., Grassian, A.R., Melman, T., Lyssiotis, C.A., Mattaini, K.R., Bass, A.J., Heffron, G., Metallo, C.M., Muranen, T., Sharfi, H., et al. (2011). Phosphoglycerate dehydrogenase diverts glycolytic flux and contributes to oncogenesis. Nat. Genet. *43*, 869–874.

Maddocks, O.D.K., Berkers, C.R., Mason, S.M., Zheng, L., Blyth, K., Gottlieb, E., and Vousden, K.H. (2013). Serine starvation induces stress and p53-dependent metabolic remodelling in cancer cells. Nature *493*, 542–546.

Maddocks, O.D.K., Labuschagne, C.F., Adams, P.D., and Vousden, K.H. (2016). Serine metabolism supports the methionine cycle and DNA/RNA methylation through de novo ATP synthesis in cancer cells. Mol. Cell *61*, 210–221.

Maguire, M., Nield, P.C., Devling, T., Jenkins, R.E., Park, B.K., Polański, R., Vlatković, N., and Boyd, M.T. (2008). MDM2 regulates dihydrofolate reductase activity through monoubiquitination. Cancer Res. *68*, 3232–3242.

Marine, J.-C., and Lozano, G. (2010). Mdm2-mediated ubiquitylation: p53 and beyond. Cell Death Differ. *17*, 93–102.

Mayo, L.D., and Donner, D.B. (2001). A phosphatidylinositol 3-kinase/Akt pathway promotes translocation of Mdm2 from the cytoplasm to the nucleus. Proc. Natl. Acad. Sci. USA *98*, 11598–11603.

Mo, P., Wang, H., Lu, H., Boyd, D.D., and Yan, C. (2010). MDM2 mediates ubiquitination and degradation of activating transcription factor 3. J. Biol. Chem. *285*, 26908–26915.

Montes de Oca Luna, R., Wagner, D.S., and Lozano, G. (1995). Rescue of early embryonic lethality in mdm2-deficient mice by deletion of p53. Nature *378*, 203–206.

Ou, Y., Wang, S.-J., Jiang, L., Zheng, B., and Gu, W. (2015). p53 Protein-mediated regulation of phosphoglycerate dehydrogenase (PHGDH) is crucial for the apoptotic response upon serine starvation. J. Biol. Chem. *290*, 457–466.

Possemato, R., Marks, K.M., Shaul, Y.D., Pacold, M.E., Kim, D., Birsoy, K., Sethumadhavan, S., Woo, H.K., Jang, H.G., Jha, A.K., et al. (2011). Functional genomics reveal that the serine synthesis pathway is essential in breast cancer. Nature *476*, 346–350.

Saiki, A.Y., Caenepeel, S., Cosgrove, E., Su, C., Boedigheimer, M., and Oliner, J.D. (2015). Identifying the determinants of response to MDM2 inhibition. Oncotarget *6*, 7701–7712.

Sullivan, L.B., Gui, D.Y., Hosios, A.M., Bush, L.N., Freinkman, E., and Vander Heiden, M.G. (2015). Supporting Aspartate Biosynthesis Is an Essential Function of Respiration in Proliferating Cells. Cell *162*, 552–563.

Toledo, F., and Wahl, G.M. (2006). Regulating the p53 pathway: in vitro hypotheses, in vivo veritas. Nat. Rev. Cancer *6*, 909–923.

Wade, M., Li, Y.-C., and Wahl, G.M. (2013). MDM2, MDMX and p53 in oncogenesis and cancer therapy. Nat. Rev. Cancer *13*, 83–96.

Watanabe, T., Hotta, T., Ichikawa, A., Kinoshita, T., Nagai, H., Uchida, T., Murate, T., and Saito, H. (1994). The MDM2 oncogene overexpression in chronic lymphocytic leukemia and low-grade lymphoma of B-cell origin. Blood *84*, 3158–3165.

Wu, L., and Levine, A.J. (1997). Differential regulation of the p21/WAF-1 and mdm2 genes after high-dose UV irradiation: p53-dependent and p53-independent regulation of the mdm2 gene. Mol. Med. *3*, 441–451.

Wysocka, J., Reilly, P.T., and Herr, W. (2001). Loss of HCF-1-chromatin association precedes temperature-induced growth arrest of tsBN67 cells. Mol. Cell. Biol. *21*, 3820–3829.

Yan, C., Lu, D., Hai, T., and Boyd, D.D. (2005). Activating transcription factor 3, a stress sensor, activates p53 by blocking its ubiquitination. EMBO J. *24*, 2425–2435.

Ye, J., Mancuso, A., Tong, X., Ward, P.S., Fan, J., Rabinowitz, J.D., and Thompson, C.B. (2012). Pyruvate kinase M2 promotes de novo serine synthesis to sustain mTORC1 activity and cell proliferation. Proc. Natl. Acad. Sci. USA *109*, 6904–6909.

Yu, Z.-C., Huang, Y.-F., and Shieh, S.-Y. (2016). Requirement for human Mps1/TTK in oxidative DNA damage repair and cell survival through MDM2 phosphorylation. Nucleic Acids Res. *44*, 1133–1150.

Zhao, E., Ding, J., Xia, Y., Liu, M., Ye, B., Choi, J.-H., Yan, C., Dong, Z., Huang, S., Zha, Y., et al. (2016). KDM4C and ATF4 Cooperate in Transcriptional Control of Amino Acid Metabolism. Cell Rep. *14*, 506–519.